THRESHOLD VOLTAGE SENSITIVITY ANALYSIS OF SURROUNDING GATE MOSFET FOR BIOSENSING APPLICATIONS

Amit Das
Maharaja Agrasen Institute of Technology
Sonam Rewari (rewarisonam@gmail.com)
Delhi Technological University Department of Electronics and Communication https://orcid.org/0000-0001-8946-9849
S.S. Deswal
Maharaja Agrasen Institute of Technology
Binod Kumar Kanaujia
Jawaharlal Nehru University
R.S. Gupta
Maharaja Agrasen Institute of Technology

Research Article

Keywords: Biosensors, Biosensing Principle, Doping, Surrounding Gate MOSFET, TCAD, Threshold Voltage

Posted Date: March 11th, 2022

DOI: https://doi.org/10.21203/rs.3.rs-1287832/v1

Abstract

A simulation based novel and unique approach of controlling and modulating the threshold voltage sensitivity of a short channel surrounding gate MOSFET biosensor is investigated for improved biosensing applications. Different results show that the biosensor with symmetric doping is more sensitive to charged and neutral biomolecules when compared with the asymmetric doping. Threshold voltage sensitivity and subthreshold slope sensitivity of 4.5 and 0.44 have been obtained which shows the significance of doping attributed sensitivity. It is so find that sensitivity increases on increasing drain to source voltage because of stronger horizontal electric field across the channel. A remarkable percentage change due to the doping variation shows the improved biosensing action in terms of threshold voltage change and subthreshold slope change.

Introduction

Field effect transistors are an important invention in the field of electronics having numerous variants used in different applications[1–6]. One of the applications which is extensively explored is biosensing[7, 8]. A good biosensor must be highly sensitive to the biomolecules. The change in the threshold voltage and subthreshold slope signifies high sensitivity. This change primarily occurs due to the filling of cavity with the biomolecules which changes the potential and electric field profile in the channel. Zahra Ahangani et. al[9] and Cong Li et. al[10] have discussed the sensitivity of biosensors in terms of threshold voltage change along with different parameter variations. Although, not much related work have been done in past[11–15]. Recently, Yogesh Pratap et. al[16] and Avik Chakraborty et.al[17] have reported surrounding gate MOSFET biosensors for the detection of biomolecule species using the different sensing metrics.

This paper gives a brilliant insight of the doping attributed sensitivity pattern in the proposed biosensor. Here, the proposed biosensor is a surrounding gate MOSFET (SG-MOSFET) with an I-shaped oxide layer and the sensitivity metrics considered are threshold voltage (V_t) and subthreshold slope (SS). The I-shaped oxide layer offers a better fill factor than its counterpart. Ehsanur Rehman et. al[18] has discussed the effect of biomolecule position and fill factor on the sensitivity of a MOSFET based biosensor. The current work and study can be generalized for similar structures of SG-MOSFET based biosensors.

First section briefly explains the literature review of the work that has been done in the past. Second section explains the device structure and methodology used. In the last section, the important results and graphs have been discussed. The main results are divided into two parts to give a better insight and comprehension of the source and drain doping dependent sensitivity pattern in the SG-MOSFET biosensor. In the first part, the doping of both source and drain is increased from a lower to a higher value at an equal rate. In the second part, a) the doping of drain is increased (keeping the doping of source and channel constant) and b), the doping of source is increased (keeping the doping of drain and channel constant).

Materials And Methods

Device structure

Figure 1 shows the 3D (three dimensional) and 2D (cross sectional) view of SG-MOSFET biosensor used for studying the doping dependent sensitivity pattern. The source and drain engineering techniques refer to the precisely varying doping of source and drain regions which gives an idea about the optimal doping over which the proposed biosensor shows the highest sensitivity.

TABLE I

STRUCTURAL PARAMETERS

Parameters	**Value**		
Channel length	30 nm		
Source/Channel/Drain radius	10 nm		
Source/Channel/Drain material	Silicon (Si)		
Work function (ψ_{gate})	4.96 eV		
Channel doping (N_C)	10^{10} /cm^3		
Source doping (N_S)	Ist Part : 10^{13} to 10^{20} /cm^3		
	IInd Part	1st Subpart : 10^{19} /cm^3	2nd Subpart : $1*10^{19}$ to $5*10^{20}$ /cm^3
Drain doping(N_D)	Ist Part : 10^{13} to 10^{20} /cm^3		
	IInd Part	1st Subpart : $1*10^{19}$ to $5*10^{20}$ /cm^3	2nd Subpart : 10^{19} /cm^3
Source/Drain length	10 nm		
Oxide layer thickness(t_{ox})	4 nm		
Cavity thickness(t_{cav})	2 nm		
Cavity length	L_1 = 14 nm		L_2 = 14 nm
Gate oxide	Silicon dioxide (SiO_2)		
Biasing	V_{DS}=0.5 V		V_{GS}=(0–1)V
Oxide length	L_{OX}= 30 nm		L_{EOX}= 2 nm
Biomolecules charge density (k_{bio}=5)	ρ= $-1*10^{11}$/cm^2 (DNA)[19]	ρ = 0 (Hydrprotein)[20]	ρ= $+1*10^{11}$ /cm^2 (Amino acids)[21]

Simulator specifications

The behavior of the proposed SG-MOSFET biosensor is studied with the mentioned parameters given in Table I on SILVACO ATLAS TCAD[22]. Different models have been incorporated for the simulation purpose: SRH model is used to support the carrier generation and recombination, CONMOB model is a mobility model and is used to relate the impurity profile with low field mobility at room temperature, FLDMOB is another field dependent mobility model. Solution method used to solve the non linear and complex differential equations is NEWTON GUMMEL method that incorporates both decoupled and coupled iterations.

Results And Discussion

Different biomolecules are characterized by their distinct dielectric constant and charge density[19, 23, 24]. Biomolecules such as 1) DNA are negatively charged (non hybridized) and can have variable charge density and dielectric constant[19] and 2) uricase, biotin, aminopropyl triethoxysilane, streptavidin, ChOx, hydroprotein, APTES are neutral biomolecules[24]. Our current work is focused upon showing the effect of source and drain doping on the sensitivity of biosensor, so we have taken biomolecules with different charge density (covering a wide range of biomolecules) which helps to study the variation of sensitivity pattern in the presence of charged biomolecules. Absence of biomolecules have been simulated by considering the cavity filled with air ($k = 1$ & $\rho = 0$).

Figure 2 shows the energy bands shifting in the SG-MOSFET at different conditions. Figure 2 (a) shows the energy bands shifting when the doping of source/drain is varied whereas Fig. 2 (b) shows the energy bands shifting in the presence of different biomolecules. High doping of source generates relatively large number of electrons compared to low doping which pulls the energy bands downward. Biomolecules inside the cavity alters the gate capacitance and lateral electric field in the channel which slightly increases the conduction band energy and valence band energy. Figure 3 shows the contour plot of electron concentration across the channel in the SG-MOSFET. Figure 3 (a) shows the electron concentration contour plot when the doping of source/drain is varied whereas Fig. 3(b) shows the electron concentration contour plot in the presence of different biomolecules. It can be clearly seen that the peak electron concentration is concentrated in the centre of the channel. Increase in the source doping increases the electron concentration (charge carriers) constituting the drain current. Presence of biomolecules inside the cavity increases the gate capacitance which changes the concentration of electrons near the Si-SiO_2 interface.

TABLE II

THRESHOLD VOLTAGE (V_T)AND THRESHOLD VOLTAGE SENSITIVITY (S_{VT}) AT DIFFERENT DOPING

Doping Value (cm^{-3}) Source_Channel_Drain		Threshold Voltage — (V_t : Volts)			Threshold Voltage Sensitivity — (S_{Vt} : Percentage)		
		k_{bio} = 5			k_{bio} = 5		
		ρ $-1*10^{11}$ cm^{-2}	ρ 0	ρ + $1*10^{11} cm^{-2}$	ρ $1*10^{11}$ cm^{-2}	ρ 0	ρ + $1*10^{11} cm^{-2}$
D_a	10^{13}_10^{10}_10^{13}	0.0459207	0.045366	0.0429468	453.0462	446.3645	417.2300
D_b	10^{14}_10^{10}_10^{14}	0.141106	0.134749	0.121702	264.6235	248.1967	214.4828
D_c	10^{15}_10^{10}_10^{15}	0.208939	0.202324	0.200550	65.7943	60.5452	59.1376
D_d	10^{16}_10^{10}_10^{16}	0.244491	0.241664	0.236106	49.4078	47.6803	44.2838
D_e	10^{17}_10^{10}_10^{17}	0.330133	0.315766	0.286625	44.9446	38.6368	25.8424
D_f	10^{18}_10^{10}_10^{18}	0.388328	0.371414	0.349767	40.7057	34.5771	26.7336
D_g	10^{19}_10^{10}_10^{19}	0.430309	0.416805	0.402911	74.1571	68.6916	63.0684
D_h	10^{20}_10^{10}_10^{20}	0.411948	0.399756	0.387387	133.8607	126.9394	119.9176

Figure 5 shows the potential profile across the channel in the SG-MOSFET. Figure 5 (a) shows the potential when the doping of source/drain is varied whereas Fig. 5(b) shows the potential in the presence of different biomolecules. Doping of source and drain changes the potential barrier at the source-channel and drain-channel junctions and this changes the potential profile across the channel. Gate capacitance and field profile changes in the presence of biomolecules which changes the channel potential. Higher doping of source and drain increases the channel potential by a considerable amount. Channel potential decreases in the presence of biomolecules which is mainly due to the change in gate oxide capacitance.

Effect of equal source and drain doping

It has been already studied that on varying the doping of source and drain at an equal rate keeping the channel doping constant will affect the sensitivity[25] of the MOSFET based biosensor. The threshold voltage depends upon various factors which can influence the sensitivity of the same[14, 15, 26].

Increasing the doping of source and drain in an identical pattern will lead to two primary effects: Effect 1 & Effect 2. When the doping of source and drain are increased at an equal rate from a low to high value, a major part of the depletion region will penetrate inside the channel than the source (source-channel junction) or drain

(drain-channel junction) which is basically the effect 1. The aggregate depletion layer width keeps on reducing with the increased doping which is basically the effect 2. So, both the effect 1 and effect 2 will be present when the doping of source and drain will be increased from a low to high value. Effect 2 is more dominant at low doping which leads to the reduction of depletion layer width and thereby increasing the effective channel length. Effect 1 is more dominant at high doping which leads to the penetration of depletion layer inside the channel resulting in the decrement of the effective channel length.

Doping notation p_q_r indicates doping of the source ($1*10^{p}$ /cm^3), channel ($1*10^{q}$ /cm^3) and drain ($1*10^{r}$ /cm^3) in the same order and the S_C_D notation indicates source_channel_drain respectively. Values of doping D_a-D_h are specified in the Table II. Both the effects will be present when the doping of source and drain is increased at an equal rate.

Table II shows the threshold voltage and threshold voltage sensitivity at different doping (equal source and drain doping) when the cavity is filled up with different biomolecules. But initially, effect 2 dominates over the effect 1 because initial increase in the doping will result in the reduction of the depletion width. This means that the depletion width keeps on reducing on both the junctions which implies that a less portion of the channel will be covered with the depletion region on both the extreme ends of the channel[27]. Therefore, the effective channel length will keep on increasing initially and hence, more gate voltage will be required to turn on the device. This implies that threshold voltage will increase when the doping of source and drain are increased initially. Now, further increasing the doping will make the effect 1 more dominant and a maximum part of the depletion region will penetrate inside the channel at both the junctions which is due to the high doping of source and drain than the doping of channel[28]. This results into the reduction of the effective channel length and hence, less gate voltage is required to turn on the device and the threshold voltage is reduced. So, the threshold voltage initially increases with the doping and attains a maximum value but after a certain doping, threshold voltage starts decreasing as shown in the Fig. 6(a). The modulus of the threshold voltage sensitivity is considered in the current study and is given in the Eq. (1).

$$S_{V_t} = \left| \left(\frac{V_{t(biomolecule)} - V_{t(air)}}{V_{t(air)}} \right) * 100 \right| \quad (1)$$

The current flowing in the biosensor is highly influenced by the biomolecules introduced in the cavity. The lateral electric field dominates and gets influenced by the biomolecules. Here, Vt_{air} and Vt_{bio} refer to the threshold voltage when the cavity is filled with air (no biomolecules) and biomolecules respectively. The threshold voltage sensitivity initially decreases until it attains a minima and then, increases in accordance with - Vt_{air} .and $|Vt_{bio} – Vt_{air}|$. Figure 6(b) and Table II also shows the threshold voltage sensitivity at different doping when the cavity is filled with biomolecules.

It has been observed that effect 2 tends to predominate at low doping [29, 30] and when source/drain doping is increased, the depletion width at both the source-channel and drain-channel junction reduces which increases the depletion capacitance (C_{dep}). The subthreshold swing is the reciprocal of the subthreshold slope[31] and is linearly proportional to C_{dep}. So, when depletion width decreases, the subthreshold swing increases but the subthreshold slope decreases at low doping [27, 28]. At high doping, effect 1 dominates

which increases the subthreshold slope. Local minima can be seen in the pattern of subthreshold slope in the Fig. 7.

Table III shows the subthreshold slope at different symmetric doping of source and drain. Subthreshold slope is influenced by the doping of source/channel/drain and the presence of biomolecules inside the cavity. Hence, subthreshold slope sensitivity (S_{SS}) first decreases until a minima is attained as $| SS_{(air)} - SS_{(bio)} |$ decreases initially where $SS_{(air)}$ and $SS_{(bio)}$ are the subthreshold slope when the cavity is filled with air and biomolecules respectively. Further increasing the doping at an equal rate increases the subthreshold slope sensitivity. This subthreshold slope sensitivity (S_{SS}) pattern can be seen in Fig. 8. Figure 8(a), 8(b) and 8(c) shows the subthreshold slope sensitivity when the cavity is filled with the negatively charged, neutral and positively charged biomolecules respectively.

Presence of charged biomolecules changes the flatband voltage which alters the potential and electric filed profile in the channel. Table III also shows the subthreshold slope sensitivity at different doping when the cavity is filled with different biomolecules. Eq. (2) shows the subthreshold slope sensitivity expression. Here, the modulus of the subthreshold slope sensitivity value is considered since sensitivity of biosensor depends upon the relative change rather than the absolute value of the metric.

$$S_{SS} = \left| \left(\frac{SS_{(air)} - SS_{(biomolecule)}}{SS_{(air)}} \right) * 100 \right| \quad (2)$$

Effect of unequal source and drain doping

Asymmetric doping of source and drain and its effect on the various sensing parameters has been critically studied[25]. For the simulation purpose, a reference doping (RD) is selected: source doping (N_S): $1*10^{19}/cm^3$, channel doping (N_C): $1*10^{10}/cm^3$, drain doping (N_D): $1*10^{19}/cm^3$. To study the effect of unequal doping, drain and source doping are varied independently. When the drain doping is increased from the reference doping, source and channel doping are kept constant & when source doping is increased from the reference doping, drain and channel doping are kept constant. Doping D_{S1}-D_{S3}, D_{RD} and D_{D1}-D_{D3} are specified in the Table IV.

If the drain doping is increased beyond the reference doping (RD), the effective channel length reduces [27, 28] and less gate voltage is required to turn on the device, i.e. the threshold voltage decreases. Figure 9 shows the variation of threshold voltage (V_t) when the cavity is filled with air and biomolecules respectively. It can be observed that the threshold voltage increases after introducing the biomolecules inside the cavity because of the strong lateral electric field developed across the channel. Due to this, the fractional change $|Vt_{(bio)} - Vt_{t(air)}| / Vt_{(air)}$ keeps on increasing with the increased drain doping. This variation of threshold voltage sensitivity (S_{Vt}) is shown in Fig. 10. As the doping of the drain keeps on increasing from the reference doping, the depletion region on the drain-channel junction keeps on penetrating inside the channel[27, 28] which results in the reduction of the depletion capacitance (C_{dep}) and this decrease in the C_{dep} decreases the subthreshold swing but increases the subthreshold slope. This pattern is shown in Fig. 11(a). The fractional change $|SS_{(air)} - SS_{(bio)}| / SS_{(air)}$ increases when the doping of the drain is further increased from the reference doping which can be seen in the Fig. 11(b).

TABLE III

SUBTHRESHOLD SLOPE (SS)AND : SUBTHRESHOLD SLOPE SENSITIVITY (S_{SS}) AT DIFFERENT DOPING

Doping Value (cm^{-3}) Source_Channel_Drain		Subthreshold Slope — (SS : $(Volts/decade)^{-1}$)			Subthreshold Slope Sensitivity — (S_{SS} : Percentage)		
		k_{bio} = 5			k_{bio} = 5		
		ρ $-1*10^{11}$ cm^{-2}	ρ 0	ρ + $1*10^{11}cm^{-2}$	ρ $1*10^{11}$ cm^{-2}	ρ 0	ρ + $1*10^{11}cm^{-2}$
D_a	$10^{13}\_10^{10}\_10^{13}$	0.07194	0.0720	0.0729	25.1176	25.0421	24.0700
D_b	$10^{14}\_10^{10}\_10^{14}$	0.07193	0.07196	0.07196	24.0830	24.0579	24.0545
D_c	$10^{15}\_10^{10}\_10^{15}$	0.07148	0.07142	0.07141	23.9825	24.0456	24.0495
D_d	$10^{16}\_10^{10}\_10^{16}$	0.07128	0.07128	0.07128	23.8258	23.8267	23.8257
D_e	$10^{17}\_10^{10}\_10^{17}$	0.07121	0.07121	0.07121	23.6722	23.6692	23.6660
D_f	$10^{18}\_10^{10}\_10^{18}$	0.07114	0.07115	0.07115	23.9660	23.9640	23.9606
D_g	$10^{19}\_10^{10}\_10^{19}$	0.07747	0.07761	0.07776	37.1150	36.9970	36.8762
D_h	$10^{20}\_10^{10}\_10^{20}$	0.09395	0.09407	0.09423	44.1769	44.1020	44.0106

With a similar discussion done above, increasing source doping leads to the reduction of the threshold voltage (V_t) which can be seen in Fig. 9. The fractional change $|Vt_{(biomolecule)} - Vt_{t(air)}|/ Vt_{(air)}$ increases with an increase in the source doping and can be seen in the Fig. 10. As the doping of the source keeps on increasing, the depletion region on the source-channel junction keeps on penetrating inside the channel. This results into the reduction of depletion capacitance (C_{dep}) which will increase the subthreshold slope and can be seen in the Fig. 11(a). The subthreshold slope sensitivity (S_{SS}) increases when the doping of the source is increased from the reference doping and is shown in the Fig. 11(b).

TABLE IV

THRESHOLD VOLTAGE SENSITIVITY & SUBTHRESHOLD SLOPE SENSITIVITY AT DIFFERENT DOPING

Doping Value (cm^{-3}) Source_Channel_Drain			Threshold Voltage Sensitivity (S_{V_t} : Percentage) — k_{bio} = 5			Subthreshold Slope Sensitivity (S_{SS} : Percentage) — k_{bio} = 5		
			ρ -1e11 cm^{-2}	ρ 0	ρ +1e11cm^{-2}	ρ -1e11 cm^{-2}	ρ 0	ρ +1e11cm^{-2}
D_{S3}	$5e10^{20}$_$1e10^{10}$_$1e10^{19}$	N_S ↑	96.4704	90.7895	85.0216	40.5620	40.4209	40.2651
D_{S2}	$1e10^{20}$_$1e10^{10}$_$1e10^{19}$		90.9764	85.4632	79.8665	39.5316	39.4166	39.3125
D_{S1}	$5e10^{19}$_$1e10^{10}$_$1e10^{19}$		87.5628	81.7503	76.6425	39.1903	39.1074	39.0235
D_{RD}	$1e10^{19}$_$1e10^{10}$_$1e10^{19}$	RD	74.1571	68.6916	63.0684	37.1150	36.9970	36.8762
D_{D1}	$1e10^{19}$_$1e10^{10}$_$5e10^{19}$	N_D ↓	95.5378	89.2265	82.7258	40.8841	40.7662	40.6425
D_{D2}	$1e10^{19}$_$1e10^{10}$_$1e10^{20}$		101.5939	95.0392	88.2835	41.4526	41.3113	41.1651
D_{D3}	$1e10^{19}$_$1e10^{10}$_$5e10^{20}$		110.4973	103.5824	96.4543	42.1210	42.0127	41.9018

Table IV shows the threshold voltage sensitivity and subthreshold slope sensitivity for different biomolecules when source and drain doping are varied at an unequal rate. Figure 12 shows the threshold voltage relative change (ΔV_t) and subthreshold slope relative change (ΔSS) at different doping when the cavity is filled with different biomolecules. A larger ΔV_t and ΔSS can be seen for negatively charged biomolecules and this change is larger at high doping. The threshold voltage offers a larger relative change and percentage sensitivity when compared to subthreshold slope, thus it can be a better sensing metric for biosensing applications. Figure 13 shows the variation of drain current with gate voltage at various doping. It can be clearly seen that drain current increases with the increased doping due to the generation of large number of charge carriers.

The prime objective of this paper is focused upon showing that the sensitivity of a biosensor is affected by the doping of the source and drain in a short channel SG-MOSFET based biosensor. Figure 14 shows the effect of drain voltage on threshold voltage sensitivity and subthreshold slope sensitivity. The effect is shown at both symmetric and asymmetric doping of source and drain. Figure 14 (a-c) shows the threshold voltage sensitivity whereas Fig. 14 (d-f) shows the subthreshold slope sensitivity. Symmetric doping (SD) considers the lower source/drain doping (N_S=10^{14}/cm^3, N_C=10^{10}/cm^3, N_D=10^{14}/cm^3) and the higher source/drain doping (N_S=10^{19}/cm^3, N_C=10^{10}/cm^3, N_D=10^{19}/cm^3) whereas asymmetric doping (ASD) considers different doping for source and drain (N_S=10^{20}/cm^3, N_C=10^{10}/cm^3, N_D=10^{19}/cm^3) for showing the effect of drain biasing on the threshold voltage sensitivity and subthreshold slope sensitivity. It can be clearly seen that both the threshold voltage sensitivity and subthreshold slope sensitivity increases with an increase in the drain voltage. Although, a higher drain voltage gives a better sensitivity but it should be noted that drain voltage cannot be increased beyond a certain limit since a high drain voltage in a short channel device may damage the device leading to its permanent breakdown.

Conclusion

This paper investigates the impact of doping on the sensitivity of the SG-MOSFET biosensor. The paper is broadly divided into two parts where source and drain doping are varied at an equal and unequal rate. Percentage sensitivity in the threshold voltage is more than the subthreshold slope which can go beyond 400% if doped at proper levels making the device more reliable and effective for biosensing applications. It is so noted that for symmetric doping, threshold voltage sensitivity is highest at low doping of source/drain (N_S=10^{14}/cm^3, N_C=10^{10}/cm^3, N_D=10^{14}/cm^3) whereas subthreshold slope sensitivity is highest at higher doping of source and drain (N_S=10^{19}/cm^3, N_C=10^{10}/cm^3, N_D=10^{19}/cm^3). Also for asymmetric doping,

threshold voltage sensitivity and subthreshold slope sensitivity is highest at higher doping of source/drain (N_S=1*10^{19}/cm^3, N_C=1*10^{10}/cm^3, N_D=5*10^{20}/cm^3). The maximum fractional sensitivity obtained for threshold voltage and subthreshold slope goes up to 4.53 and 0.44 respectively for equal source and drain doping whereas the maximum sensitivity obtained for threshold voltage and subthreshold slope goes up to 1.10 and 0.42 for unequal source and drain doping. Here, the symmetric doping of drain and source has shown larger sensitivity in terms of threshold voltage change and subthreshold voltage change when compared to the asymmetric doping of drain and source. It's evident that doping also plays an important role in controlling the achieved sensitivity of short channel MOSFET based biosensors. Nevertheless, this paper laid down a unique and basic framework for further study on doping dependent sensitivity of similar biosensors.

Declarations

Acknowledgement

Authors are grateful to the Director, Maharaja Agrasen Institute of Technology, Delhi for providing the facilities to carry out this research work. One of the author (Amit Das) would like to thank UGC, Government of India for financial assistance to carry out this research work.

References

1. Upasana, Narang R, Saxena M, Gupta M (2015) Modeling and TCAD assessment for gate material and gate dielectric engineered TFET architectures: Circuit-level investigation for digital applications. IEEE Trans Electron Devices 62:3348–3356. https://doi.org/10.1109/TED.2015.2462743
2. Sirohi A, Sahu C, Singh J (2019) Analog/RF Performance Investigation of Dopingless FET for Ultra-Low Power Applications. IEEE Access 7:141810–141816. https://doi.org/10.1109/ACCESS.2019.2937444
3. Park J, Hiep H, Woubit A, Kim M (2014) Applications of Field-Effect Transistor (FET) -Type Biosensors. 23:61–71
4. Das A, Kanaujia BK, Nath V et al (2020) Impact of Reverse Gate Oxide Stacking on Gate All Around Tunnel FET for High Frequency Analog and RF Applications. In: IEEE 17th India Council International Conference (INDICON). pp 1–6
5. Gautam R, Saxena M, Gupta RS, Gupta M (2013) Gate-all-around nanowire MOSFET with catalytic metal gate for gas sensing applications. IEEE Trans Nanotechnol 12:939–944. https://doi.org/10.1109/TNANO.2013.2276394
6. Kumar M, Haldar S, Gupta M, Gupta RS (2014) Impact of gate material engineering(GME) on analog/RF performance of nanowire Schottky-barrier gate all around (GAA) MOSFET for low power wireless applications: 3D T-CAD simulation. Microelectron J. https://doi.org/10.1016/j.mejo.2014.07.010
7. Kaisti M (2017) Detection principles of biological and chemical FET sensors. Biosens Bioelectron 98:437–448. https://doi.org/10.1016/j.bios.2017.07.010
8. Das A, Rewari S, Kanaujia BK, Gupta RS (2021) Recent Technological Advancement in Surrounding Gate MOSFET for Biosensing Applications - a Synoptic Study.Silicon13

9. Ahangari Z (2016) Performance assessment of dual material gate dielectric modulated nanowire junctionless MOSFET for ultrasensitive detection of biomolecules. RSC Adv 6:89185–89191. https://doi.org/10.1039/c6ra17361f
10. Li C, Liu F, Han R, Zhuang Y (2021) A Vertically Stacked Nanosheet Gate-All-Around FET for Biosensing Application. IEEE Access 9:63602–63610. https://doi.org/10.1109/ACCESS.2021.3074906
11. Li J, Zhang Y, To S et al (2011) Effect of nanowire number, diameter, and doping density on nano-FET biosensor sensitivity. ACS Nano 5:6661–6668. https://doi.org/10.1021/nn202182p
12. Chiang MH, Lin CN, Lin GS (2006) Threshold voltage sensitivity to doping density in extremely scaled MOSFETs. Semicond Sci Technol 21:190–193. https://doi.org/10.1088/0268-1242/21/2/017
13. Fathil MFM, Tamjis N, Arshad MKM et al (2018) The impact of different channel doping concentrations on the performance of polycrystalline silicon nanowire field-effect transistor biosensor. https://doi.org/10.1063/1.5080819. AIP Conf Proc 2045:
14. Iménez A, Ambrosio RC, Mireles J et al (2013) Analysis of threshold voltage fluctuations due to short channel and random doping effects. Superf y Vacio 26:1–3
15. Jung H-K (2011) Analysis of Doping Profile Dependent Threshold Voltage for DGMOSFET Using Gaussian Function. J Inf Commun Converg Eng 9:310–314. https://doi.org/10.6109/jicce.2011.9.3.310
16. Pratap Y, Kumar M, Kabra S et al (2018) Analytical modeling of gate-all-around junctionless transistor based biosensors for detection of neutral biomolecule species.J Comput Electron
17. Chakraborty A, Sarkar A (2017) Analytical modeling and sensitivity analysis of dielectric-modulated junctionless gate stack surrounding gate MOSFET (JLGSSRG) for application as biosensor. J Comput Electron 16:556–567
18. Rahman E, Shadman A, Khosru QDM (2017) Effect of biomolecule position and fill in factor on sensitivity of a Dielectric Modulated Double Gate Junctionless MOSFET biosensor. Sens Bio-Sensing Res 13:49–54
19. Lodhi A, Rajan C, Kumar A et al (2020) Sensitivity and sensing speed analysis of extended nano – cavity and source over electrode in Si / SiGe based TFET biosensor. Appl Phys A 126:1–8. https://doi.org/10.1007/s00339-020-04008-0
20. Goel A, Rewari S, Verma S et al (2021) Dielectric Modulated Junctionless Biotube FET (DM-JL-BT-FET) Bio-Sensor. IEEE Sens J 21:16731–16743. https://doi.org/10.1109/JSEN.2021.3077540
21. Rosini E, D'antona P, Pollegioni L (2020) Biosensors for d-amino acids: Detection methods and applications. Int J Mol Sci 21. https://doi.org/10.3390/ijms21134574
22. Software DS (2018) ATLAS User's Manual Device Simulation Software Volume I. I:318
23. Kim C-H, Jung C, Park HG, Choi Y-K (2008) Novel Dielectric-Modulated Field-Effect Transistor for Label-Free DNA Detection. BioChip 2:127–134
24. Pratap Y, Kumar M, Kabra S et al (2018) Analytical modeling of gate-all-around junctionless transistor based biosensors for detection of neutral biomolecule species. J Comput Electron 17:288–296
25. Sun K, Zeimpekis I, Hu C et al (2016) Effect of subthreshold slope on the sensitivity of nanoribbon sensors. Nanotechnology 27. https://doi.org/10.1088/0957-4484/27/28/285501
26. Zhou H (2014) Florida State University Libraries Analysis of Threshold Voltage Fluctuations. Induced by Random Doping in MOSFET

27. Kang S-M, Yusuf L (2003) CMOS Digital Integrated Circuits, 3rd ed
28. Adel SS, C.Smith K (2020) Microelectronics Circuit, 8th ed. Oxford
29. Beckers A, Jazaeri F, Enz C (2019) Theoretical Limit of Low Temperature Subthreshold Swing in Field-Effect Transistors. IEEE Electron Device Lett 41:1. https://doi.org/10.1109/LED.2019.2963379
30. Kobayashi M (2018) A perspective on steep-subthreshold-slope negative-capacitance field-effect transistor.Appl Phys Express11
31. Tiwari PK, Panda CR, Agarwal A et al (2010) Modelling of doping-dependent subthreshold swing of symmetric double-gate MOSFETs. IET Circuits Devices Syst 4:337–345. https://doi.org/10.1049/iet-cds.2009.0201

Figures

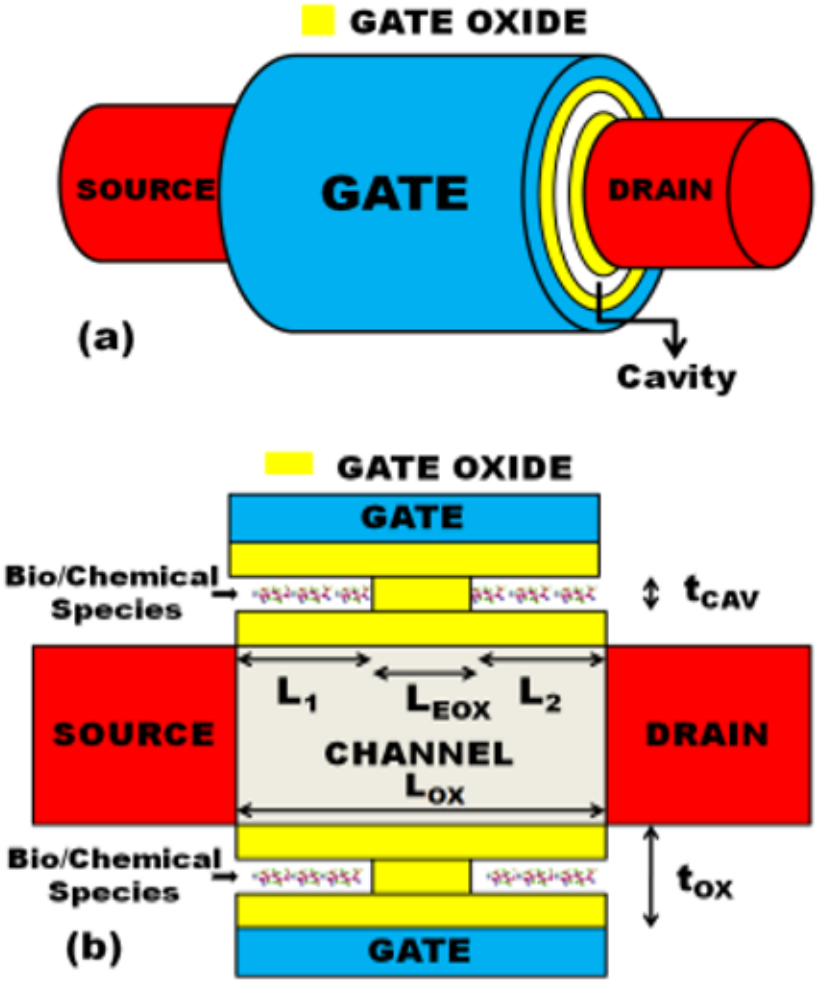

Figure 1

(a) 3D view and **(b)** 2D view of SG-MOSFET biosensor

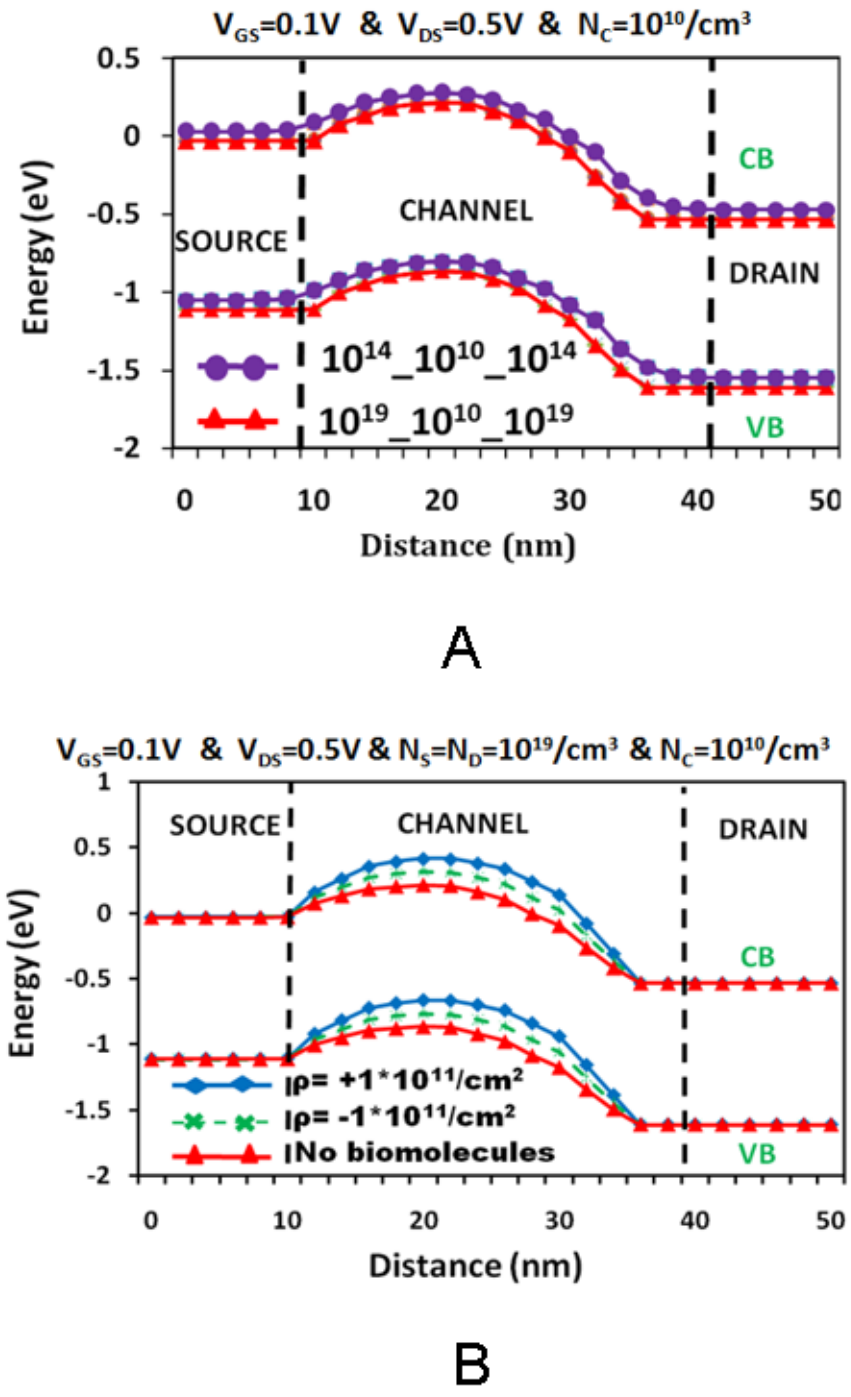

Figure 2

(a) Energy band diagram at different source/drain doping in the SG-MOSFET biosensor **(b)** Energy bands shifting in the presence of different biomolecules in the SG-MOSFET biosensor (k_{bio}=5 & N_C=10^{10}/cm^3)

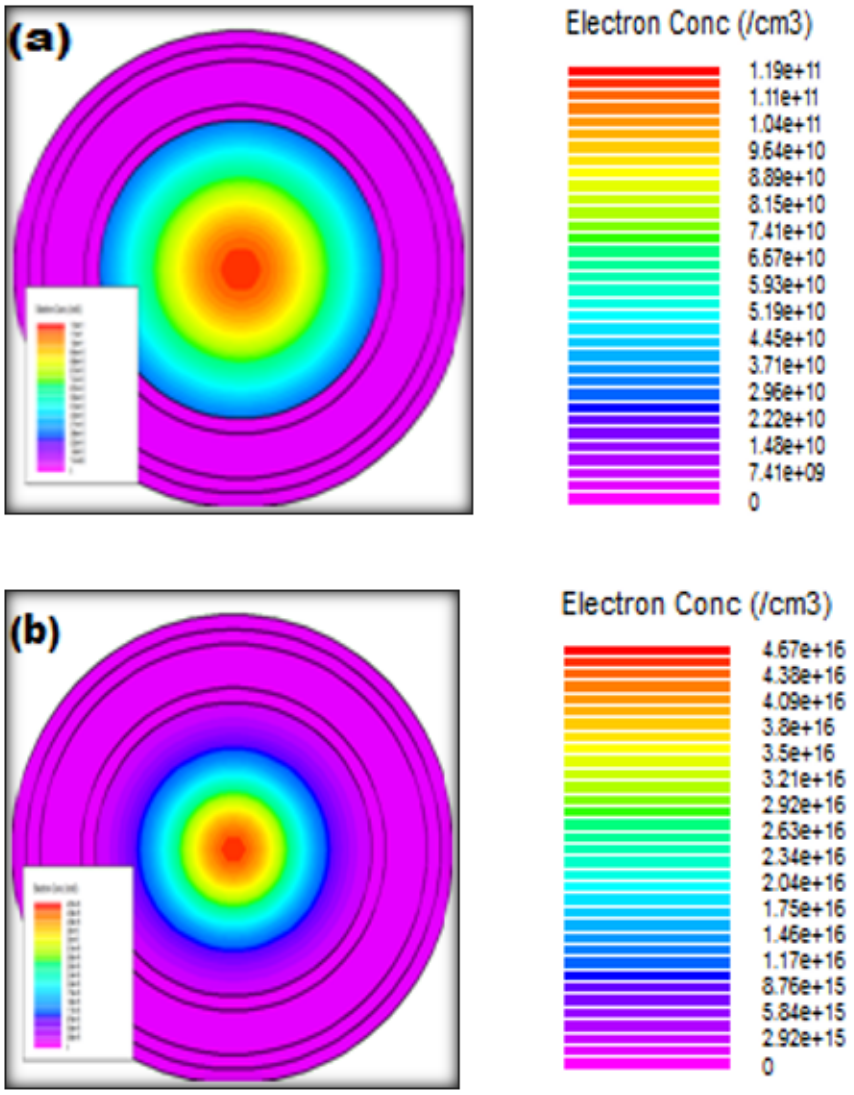

Figure 3

Electron concentration contour plot (V_{GS}=0.1V and V_{DS}=0.5V) at **(a)** $N_S=N_D=10^{14}$ /cm^3 , $N_C=10^{10}/cm^3$ and **(b)** $N_S=N_D=10^{19}$ /cm^3 , $N_C=10^{10}/cm^3$ in the SG-MOSFET biosensor

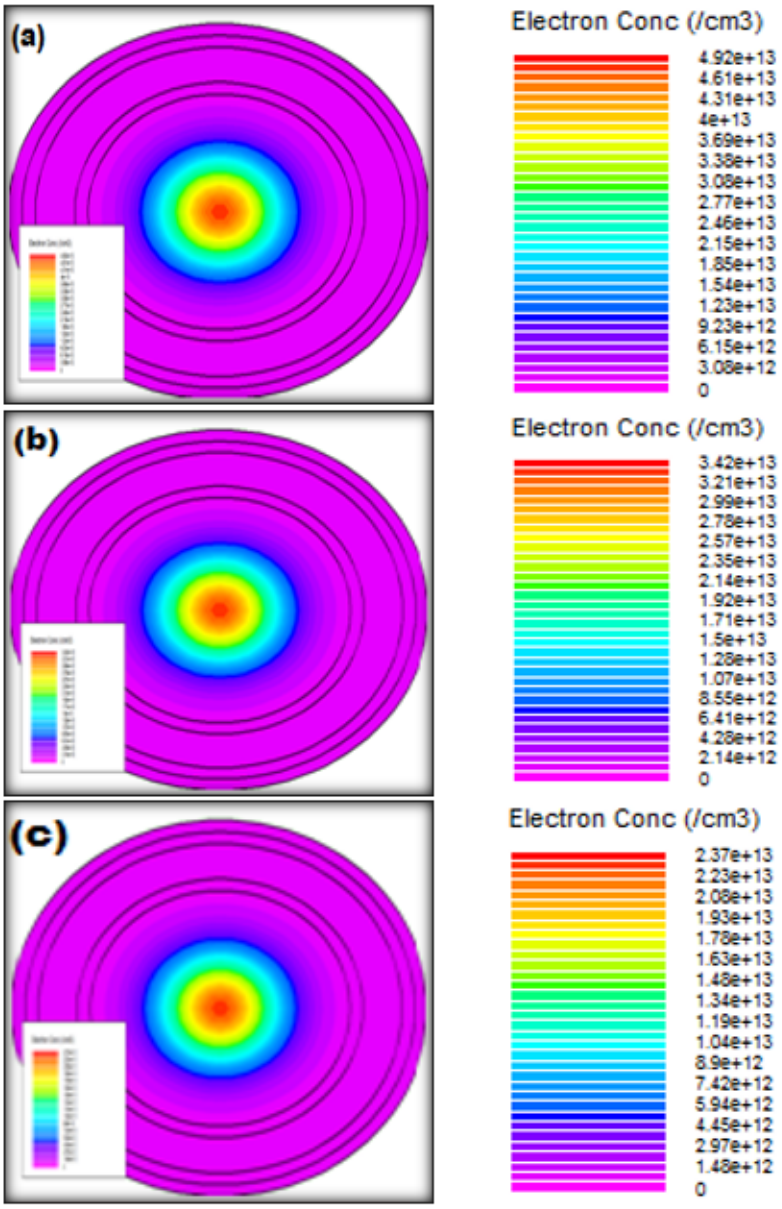

Figure 4

Electron concentration contour plot (V_{GS}=0.1V, V_{DS}=0.5V , k_{bio}=5 N_S=N_D=10^{19} /cm^3 & N_C=10^{10}/cm^3) at different charge density **(a)** ρ=1*10^{11} / cm^2 , **(b)** ρ=0 and **(c)** ρ=1*10^{11} / cm^2 of biomolecules in the SG-MOSFET biosensor

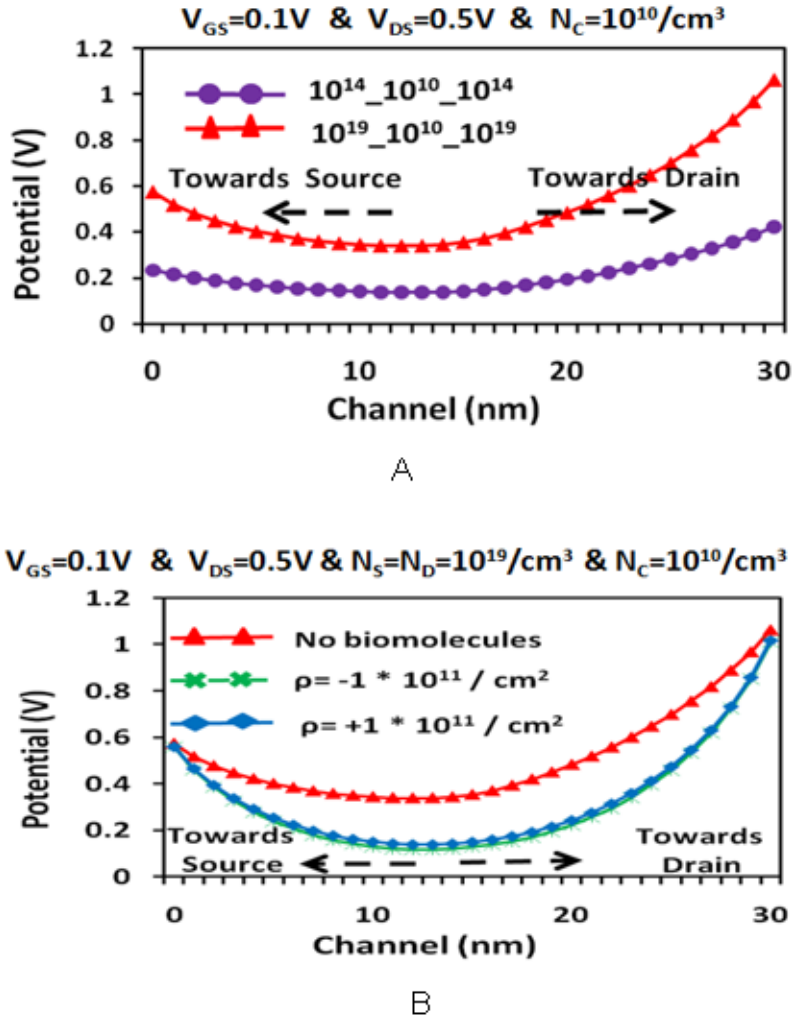

Figure 5

(a) Potential profile across the channel at different source/drain doping in the SG-MOSFET biosensor **(b)** Potential profile across the channel in the presence of different biomolecules in SG-MOSFET biosensor (V_{GS}=0.1V, k_{bio}=5 & V_{DS}=0.5V)

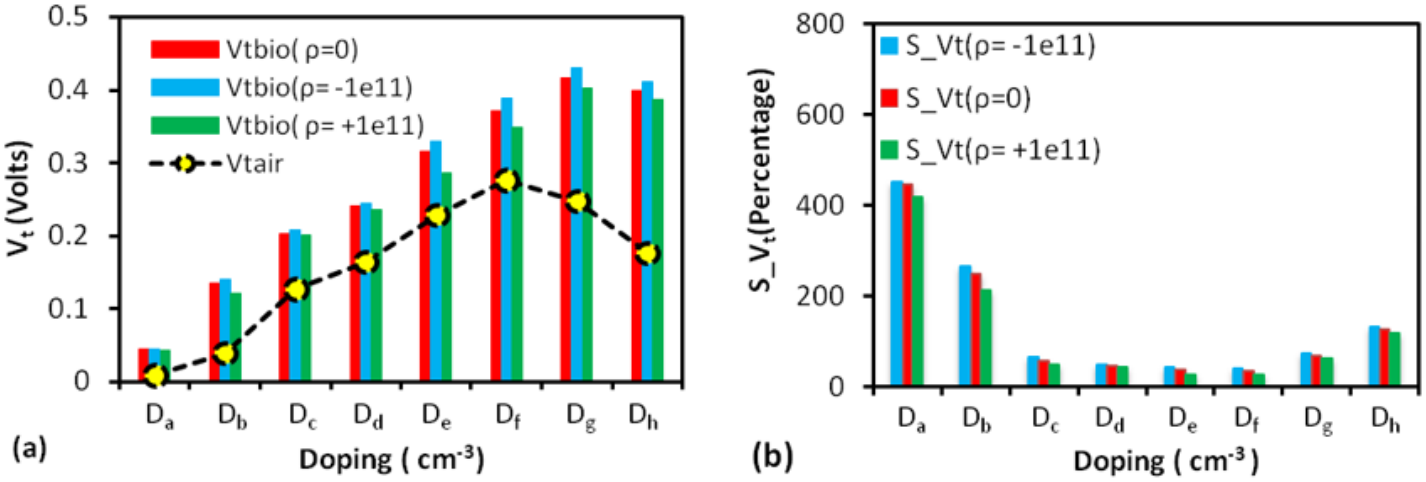

Figure 6

(a) Threshold voltage (V_t) and **(b)** threshold voltage sensitivity (S_Vt) in the SG-MOSFET biosensor when the cavity is filled with biomolecules at different doping (V_{DS}=0.5V, N_C=10^{10}/cm^3 & k_{bio}=5)

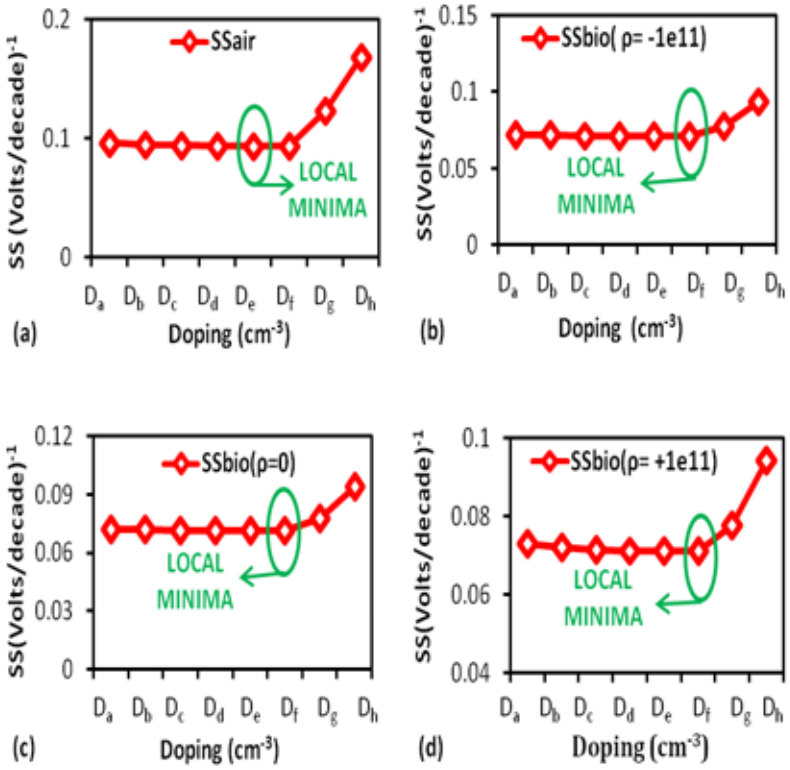

Figure 7

Subthreshold slope (SS) in the SG-MOSFET biosensor when the cavity is filled with **(a)** air, **(b)** negatively charged (ρ= -1e11/ cm^2) biomolecules, **(c)** neutral biomolecules (ρ=0) and **(d)** positively charged (ρ= +1e11/

cm^2) biomolecules at different doping (V_{DS}=0.5V, N_C=10^{10}/cm^3 & k_{bio}=5)

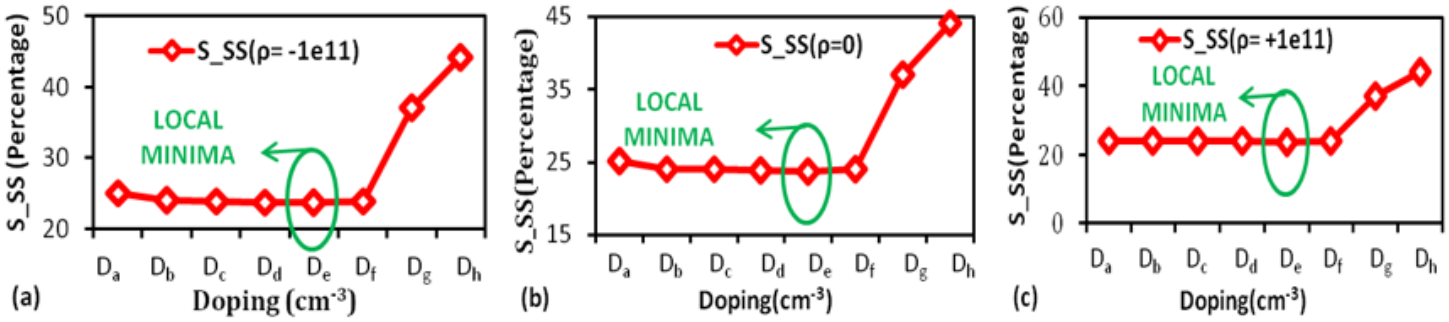

Figure 8

Subthreshold slope sensitivity (S_SS) in the SG-MOSFET biosensor when the cavity is filled with **(a)** negatively charged biomolecules (ρ= -1e11/ cm^2), **(b)** neutral (ρ= 0) biomolecules and **(c)** positively charged (ρ= +1e11/ cm^2) biomolecules at different doping (V_{DS}=0.5V, N_C=10^{10}/cm^3 & k_{bio}=5)

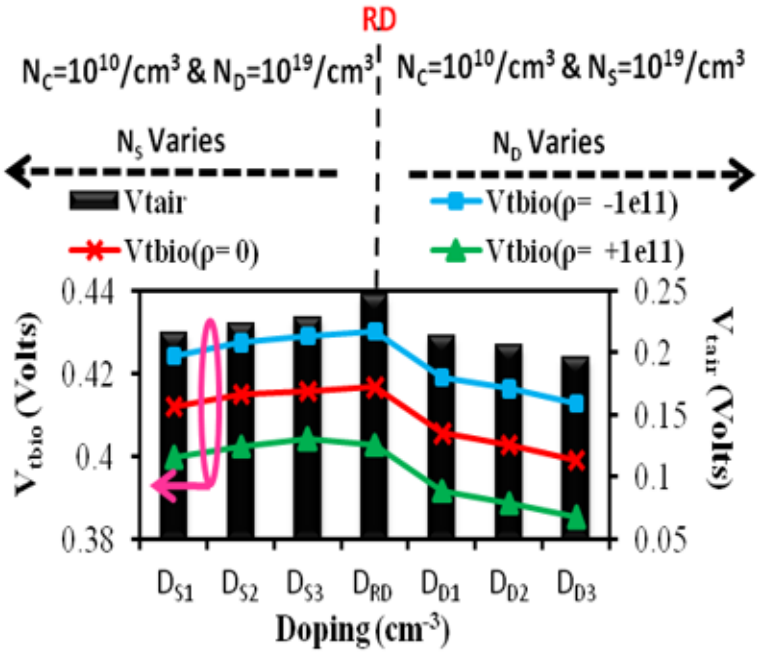

Figure 9

Threshold voltage (V_t) in the SG-MOSFET biosensor when the cavity is filled with air and biomolecules (V_{DS}=0.5V, N_C=10^{10}/cm^3 & k_{bio}=5)

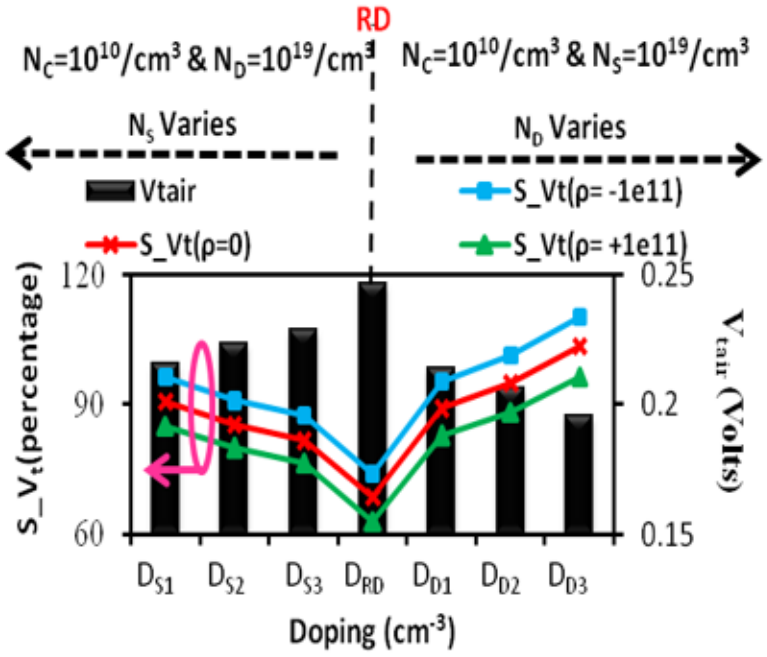

Figure 10

Threshold voltage sensitivity (S_Vt) in the SG-MOSFET biosensor when the cavity is filled with biomolecules (V_{DS}=0.5V, $N_C=10^{10}/cm^3$ & k_{bio}=5)

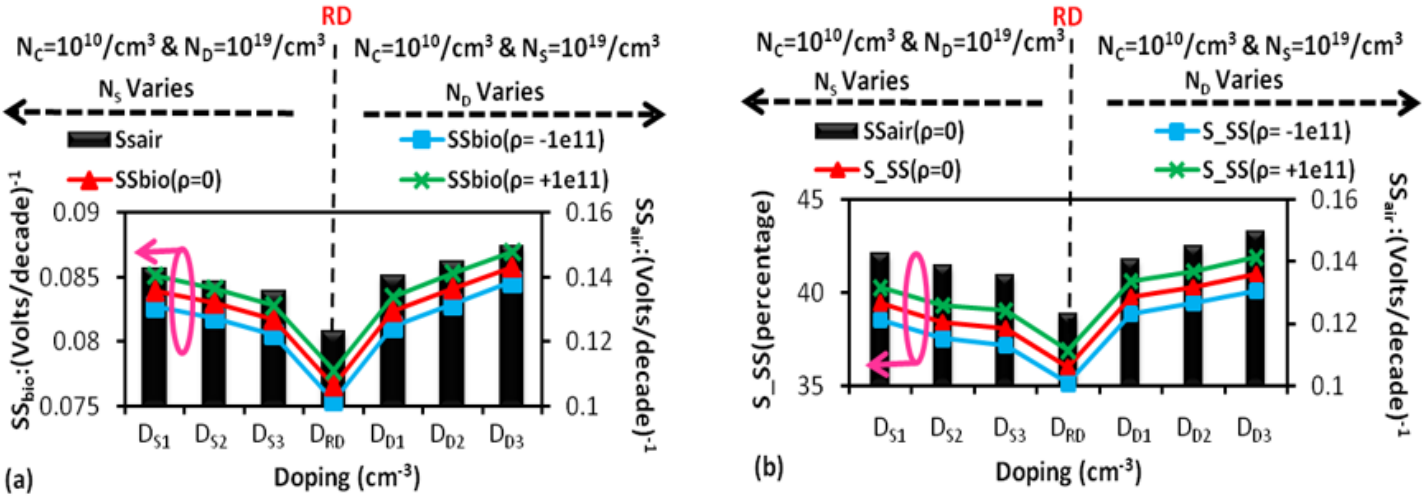

Figure 11

(a) Subthreshold slope (SS) and **(b)** subthreshold slope sensitivity (S_SS) in the SG-MOSFET biosensor when the cavity is filled with biomolecules (V_{DS}=0.5V, $N_C=10^{10}/cm^3$ & k_{bio}=5)

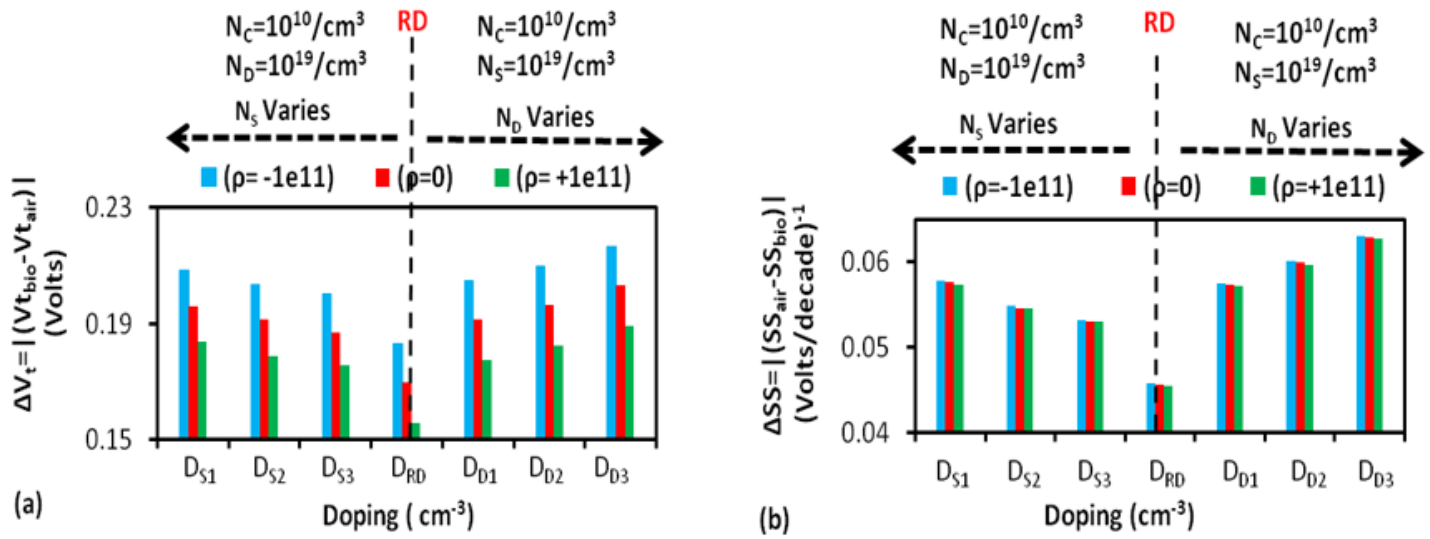

Figure 12

(a) Threshold voltage change (ΔVt) and **(b)** subthreshold slope change (ΔSS) when the cavity is filled with biomolecules at different doping (V_{DS}=0.5V, $N_C=10^{10}/cm^3$ & k_{bio}=5)

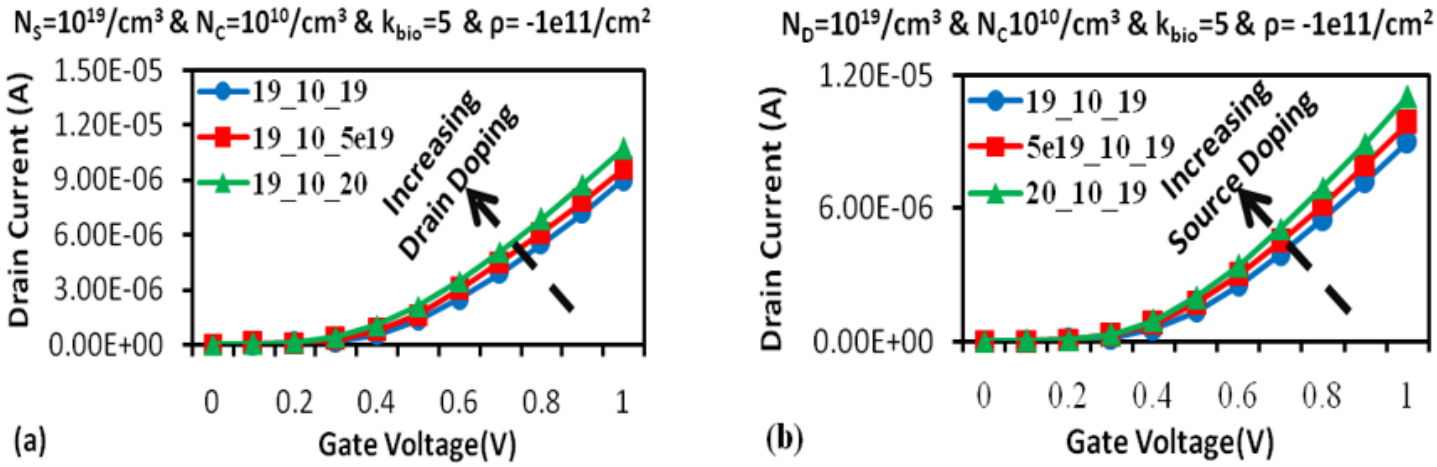

Figure 13

Drain current (I_{DS}) variation with the gate voltage (V_{GS}) at different (a) drain doping ($N_C=10^{10}/cm^3$ & $N_S=10^{19}/cm^3$) and (b) source doping ($N_C=10^{10}/cm^3$ & $N_D=10^{19}/cm^3$) at V_{DS}=0.5V, k_{bio}=5 and ρ= -1e11/ cm^2

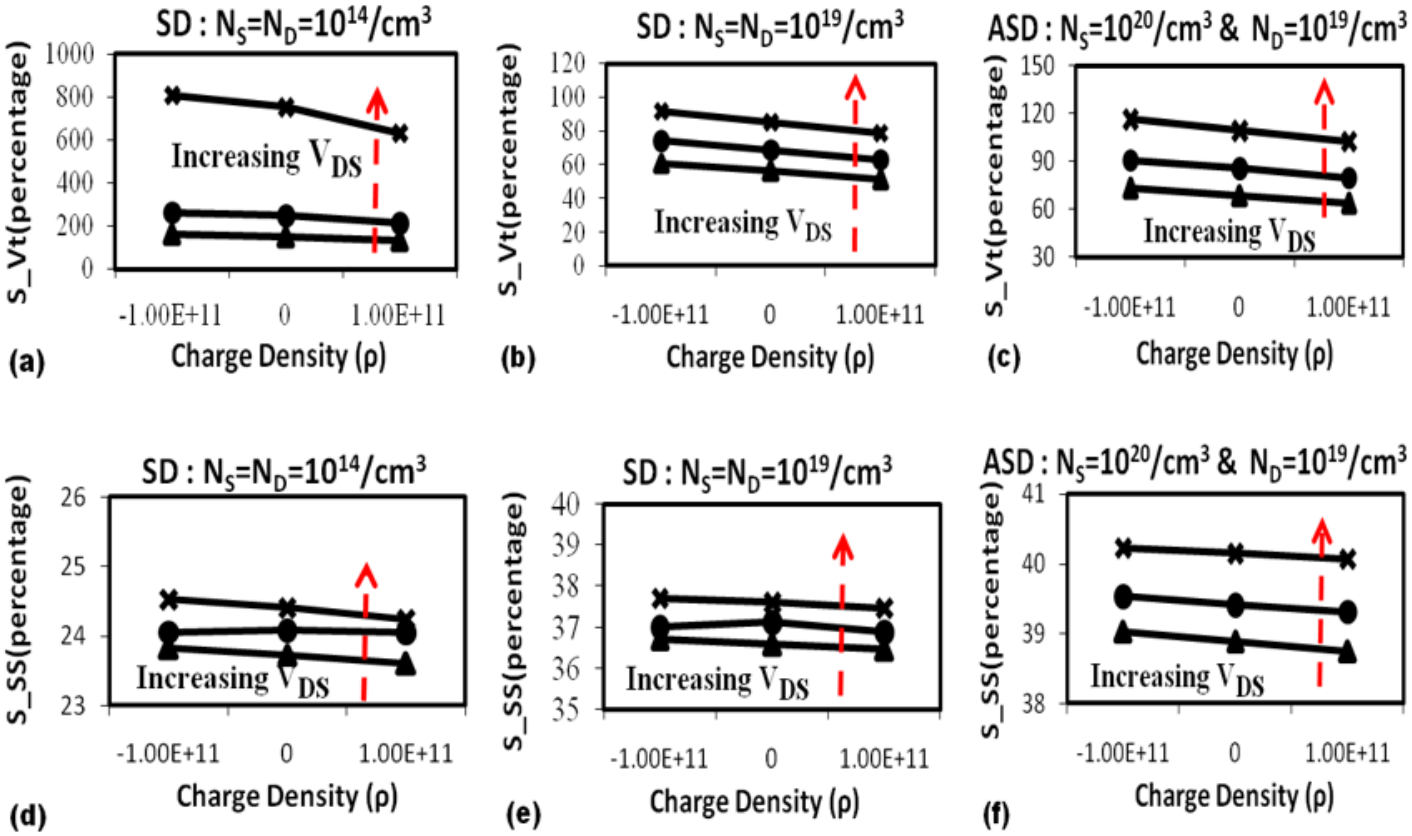

Figure 14

Effect of drain voltage on **(a-c)** threshold voltage sensitivity (S_Vt) and **(d-f)** subthreshold slope sensitivity (S_SS) at different doping ($N_C=10^{10}/cm^3$and $k_{bio}=5$)